Fault-Tolerant Control of a Dual Three-Phase Interior PMSM Under Open-Phase Faults

Marcos Orviz
Dept of Elect. Computer & System Engineering, University of Oviedo
Gijón, 33204, Spain
orvizmarcos@uniovi.es

Diego F. Laborda
Dept of Elect. Computer & System Engineering, University of Oviedo
Gijón, 33204, Spain
dflaborda@uniovi.es

Juan Manuel Guerrero
Dept of Elect. Computer & System Engineering, University of Oviedo
Gijón, 33204, Spain
guerrero@uniovi.es

David Reigosa
Dept of Elect. Computer & System Engineering, University of Oviedo
Gijón, 33204, Spain
diazdavid@uniovi.es

***Abstract*—Conventional three-phase machines are being substituted by multi-phase ones in certain applications due to their improved fault-tolerant capability, which is typically achieved through a modified control strategy. Dual three-phase permanent magnet synchronous machines (DT-PMSMs) with isolated neutral points are advantageous from the point of view of control simplicity as they avoid the flow of zero-sequence currents. Fault-tolerant control (FTC) strategies under open-phase faults have been already proposed for surface DT-PMSMs, but the extension of these techniques to flux-weakening (FW) and maximum torque per ampere (MTPA) operation of interior DT-PMSMs (DT-IPMSMs) is not possible. This paper will both extend a previous FTC strategy and propose a novel one, both of them allowing FW and MTPA operation in a DT-IPMSM after an open-phase fault.[1]**

Keywords—multi-phase, fault-tolerant control, open-phase, flux-weakening.

I. Introduction

In recent years, the use of permanent magnet synchronous machines (PMSMs) has extensively increased in both traction and industrial applications, as they outperform other types of electric machines in terms of power and torque densities, controllability, and efficiency. Although most of PMSMs are three-phase machines, the use of multi-phase machines (i.e., with a higher number of phases) provides several advantages, especially in aspects related to the fault-tolerant capability of the machine [1]. Therefore, for certain applications in which the reliability of the drive is essential, the conventional three-phase variable speed drives are being substituted by multi-phase ones [1]-[15].

Multi-phase PMSMs can be divided into those the number of phases is not a multiple of three (e.g., five-phase [2], seven-phase [3], or eleven-phase [4]) and those with the number of phases being a multiple of three. The latter can be further divided into those without independent three-phase windings (e.g., six-phase [5] or nine-phase [6]) and those in which multiple independent three-phase windings can be distinguished (e.g., dual three-phase [7] or triple three-phase [8]).

Multi-phase PMSMs with independent three-phase winding sets are advantageous from the point of view of control simplicity since the conventional three-phase control can be easily extended. In addition, the use of conventional three-phase converters is possible. Among them, dual three-phase PMSMs (DT-PMSMs) consist of a combination of two sets of three-phase windings shifted 30 (asymmetrical) or 60 (symmetrical) electrical degrees [7]. Both three-phase sets can be isolated or connected through their neutral points. Connected neutral points provide improved fault-tolerant capability (one extra degree of freedom) but increase the control complexity. Isolated neutral points avoid the flow of zero-sequence currents, thus easing the machine control [9].

Typically, the fault-tolerant capability of a multi-phase machine is achieved through a modified control strategy (i.e., a fault-tolerant control (FTC) strategy). Open-phase faults are one of the most common faults in electrical drives [1]. The goal of FTC strategies under open-phase faults is to take advantage of the healthy phases to keep the machine operating with reduced torque pulsations. In a DT-PMSM, the simplest way of achieving this goal is removing the faulty three-phase set making the machine operate only with the healthy winding. However, this would halve the torque capability of the machine. In [10]-[12] vector space decomposition (VSD) theory is applied in a DT-PMSM to keep the machine operating under an open-phase fault. These methods require the use of additional transformation matrices (to distinguish between different subspaces). Moreover, additional current controllers need to be implemented to regulate the harmonic subspace currents. The use of additional proportional-integral (PI) [10], PI plus proportional-resonant (PR) [11] and deadbeat [12] controllers has been reported for this purpose. A genetic algorithm (GA) was used in [13] to maximize torque output and minimize torque and speed ripple under open-phase faults in a DT-PMSM; the method is valid for both interior and surface PMSMs. However, the need of developing a GA to optimize the generation of current references during fault operation increases the implementation complexity of the technique while placing concern on the computational burden. In [14], a constant average q-axis current reference with superimposed pulsations is commanded in the faulty winding since, when working in two-phase mode, pulsations around the constant q-axis current reference are unavoidable. To compensate for that pulsations, opposite current references are used in the healthy winding. In this way, pulsations are removed from the total q-axis current (i.e., the sum of the q-axis current of each three-phase set). A DT-PMSM with isolated windings driven by two three-leg inverters (one per three-phase winding) was used for this purpose. This method was extended in [15] to maximize the torque output. However, those techniques require zero total d-axis current (average). Besides, synchronous PI controllers (in rotor reference frame) were used to control the pulsating dq-axes currents, whose performance is drastically reduced at high speeds (higher frequency of current pulsations).

[1]This work was supported in part by the Research, Technological Development and Innovation Programs of the Spanish Ministry of Science and Innovation, under grant PID2019-106057RB-I00.

In this paper the FTC strategy proposed in [14] will be extended to allow injection of average *d*-axis current different from zero and without pulsations, enabling maximum torque per ampere (MTPA) and flux weakening (FW) operation of a dual three-phase interior PMSM (DT-IPMSM). In addition, a new FTC strategy based on varying the current reference of the healthy three-phase set depending on the faulty three-phase winding current measurements will be proposed. Additional PI controllers will be included to control specific frequency components ($\pm 2\omega r$, and $\pm 4\omega r$, depending on the selected method) of the current.

The paper is organized as follows: Section II presents the proposed FTC techniques; their implementation is discussed in Section III. Simulation results are included in Section IV. Conclusions are finally given in Section V.

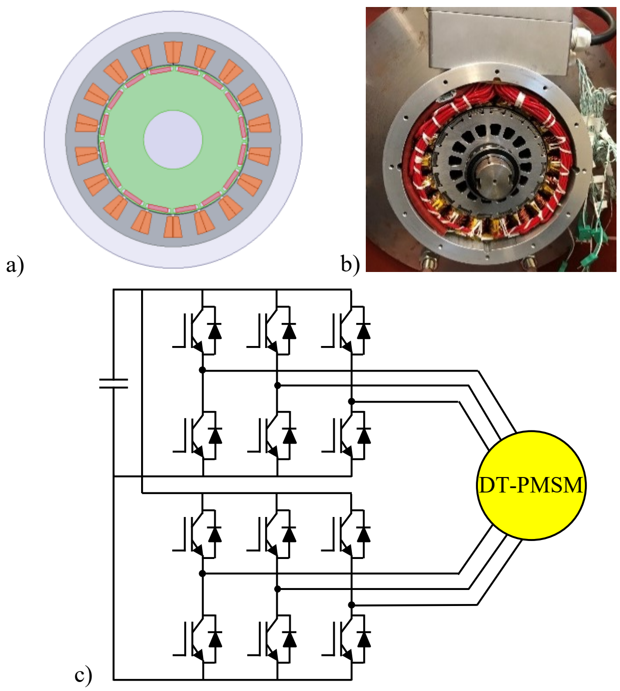

Fig. 1: Test machine a) 2D model, b) picture and c) drive

Table I: Test Machine Characteristics	
Machine type	DT-IPMSM
Number of stator slots	18
Number of rotor pole pairs	8
Rated Current	10 A
Rated Speed	1125 rpm

II. Machine Design and FTC Methods

Fig. 1a-b shows a 2D model and a picture of the test machine, its main characteristics being shown in Table I. The three-phase windings have isolated neutral points and are shifted by 60 electrical degrees. Each three-phase winding set will be driven by an independent three-leg inverter (see Fig. 1c). This machine drive configuration allows to independently control each three-phase winding. Therefore, if one inverter suffers an open-phase fault, the current pulsations produced in the faulty winding can be compensated by the healthy one [14],[15]. The torque equation for this machine is shown in (1), where P is the pole pair number, λ_{PM} is the PM flux linkage, L_d and L_q are the *dq*-axes inductances, which are assumed to be equal in both three-phase sets, and i_{d1}, i_{q1}, i_{d2}, and i_{q2} are the *dq*-axes currents of three-phase sets 1 (phases a-b-c) and 2 (phases d-e-f), respectively. Based on this fact, this section develops two different FTC strategies under an open-phase fault: the first method (Method 1) controls the *dq*-axes currents in both the faulty and the healthy three-phase sets to obtain a total *dq*-axes current without pulsations; the second method (Method 2) applies the FTC strategy only in the healthy three-phase winding, i.e., no FTC strategy is applied in the faulty set after the fault.

$$T=1.5P\left[\lambda_{PM}\left(i_{q1}+i_{q2}\right)+\left(L_d-L_q\right)\left(i_{d1}i_{q1}+i_{d2}i_{q2}\right)\right] \tag{1}$$

$$i_{d1}=2/3[i_a\cdot\cos(\omega_r t)+i_b\cdot\cos(\omega_r t-2\pi/3) +i_c\cdot\cos(\omega_r t+2\pi/3)] \tag{2}$$

$$i_{q1}=2/3[i_a\cdot\sin(\omega_r t)+i_b\cdot\sin(\omega_r t-2\pi/3) +i_c\cdot\sin(\omega_r t+2\pi/3)] \tag{3}$$

$$i_{d1}=\left(2\sqrt{3}/3\right)\cdot I\cdot\sin(\omega_r t) \tag{4}$$

$$i_{q1}=\left(2\sqrt{3}/3\right)\cdot I\cdot\cos(\omega_r t) \tag{5}$$

A. Method 1

Equations (2) and (3) show the three-phase to synchronous reference frame transformation of the currents for three-phase winding 1. Assuming an open-phase fault in phase-a: ia = 0 and ib = -ic = I, (2) and (3) can be simplified to (4) and (5). The FTC ideal goal would be to modulate the phase current, I, to obtain a dc value for both i_{d1} and i_{q1}. However, this is not feasible in practice, as (4) and (5) necessarily must be zero for some rotor angle. Therefore, the goal of the proposed FTC strategy will be to find a phase current, I, leading to an average value of i_{d1} and i_{q1} different from zero. If $I=A\cdot\sin(\omega_r t+\phi)$, where A indicates the amplitude of the phase current and ϕ its phase shift, (4) and (5) can be written as in (6) and (7), where $k=A/\sqrt{3}$. It can be observed that the resulting *dq*-axes currents under an open-phase fault in the three-phase winding 1, i_{d1} and i_{q1}, have two different terms, one dc component, and one component rotating at twice the fundamental frequency, $2\omega_r$. Thus, to obtain total *dq*-axes currents (i.e., $i_{dT} = i_{d1}+i_{d2}$ and $i_{qT} = i_{q1}+i_{q2}$) without pulsations, the component at $2\omega_r$ must be compensated in the healthy winding (three-phase set 2), see (8) and (9). Finally, (10) and (11) show the total *dq*-axes currents under an open-phase fault in phase-a, applying the proposed FTC strategy. It can be seen that the current pulsations have been removed and the amplitude and angle of the *dq*-complex vector are controlled with k and ϕ, respectively. Therefore, (6)-(9) will provide the new current references for both three-phase windings during an open phase fault in phase-a.

$$i_{d1}=k\cdot\cos(\phi)-k\cdot\cos(2\omega_r t+\phi) \tag{6}$$

$$i_{q1}=k\cdot\sin(\phi)+k\cdot\sin(2\omega_r t+\phi) \tag{7}$$

$$i_{d2}=k\cdot\cos(\phi)+k\cdot\cos(2\omega_r t+\phi) \tag{8}$$

$$i_{q2}=k\cdot\sin(\phi)-k\cdot\sin(2\omega_r t+\phi) \tag{9}$$

$$i_{dT}=2k\cdot\cos(\phi) \tag{10}$$

$$i_{qT}=2k\cdot \sin(\phi) \quad (11)$$

B. Method 2

When a DT-IPMSM is running in healthy operation, the *dq*-axes currents of each three-phase winding are often controlled to follow a certain dc command tracked with synchronous, PI controllers. However, if one of the phases suffers an open-phase fault, the PI controllers will not be able to avoid the appearance of current pulsations around the dc command. The controller error can be expressed as in (12) and (13), where i_{d1}*, i_{q1}*, i_{d1}, and i_{q1} are the *dq*-axes current commands and actual currents in the faulty three-phase winding, respectively. To compensate for the current errors in the faulty three-phase set, *dq*-axes current commands in the healthy winding (three-phase set 2) can be adapted based on the faulty three-phase set current error. Equations (14) and (15) show the new current commands in the healthy three-phase set after an open-phase fault, i_{d2_FT}* and i_{q2_FT}*, where i_{d2} * and i_{q2} * are the current references in the same three-phase set before the open-phase fault. In this way, the controller error in the faulty three-phase set will be compensated with the healthy one, the total *dq*-axes currents being identical before and after the fault.

$$ei_{d1}=i^*_{d1}-i_{d1} \quad (12)$$

$$ei_{q1}=i^*_{q1}-i_{q1} \quad (13)$$

$$i^*_{d2FT}=i^*_{d2}+ei_{d1} \quad (14)$$

$$i^*_{q2FT}=i^*_{q2}+ei_{q1} \quad (15)$$

III. Implementation

Fig. 2 shows the block diagram for the implementation of the proposed FTC techniques (Method 1 and Method 2). The inputs of the block diagram are the current references of both three-phase sets in the synchronous reference frame, i^*_{dq1} and i^*_{dq2} during the healthy operation of the machine. In the event of an open-phase fault in one of the machine phases, the current references will be recalculated using Method 1 [see (6)-(9)] or Method 2 [see (14)-(15)] to compensate for the current pulsations provoked by the fault. Thus, $i^*_{dq1\_FT}$ and $i^*_{dq2\_FT}$ are obtained. After that, current regulators will be used to track the current references. PI controllers are often used for this purpose. However, since $i^*_{dq1\_FT}$ and $i^*_{dq2\_FT}$ include additional frequency components (apart from the fundamental one), the use of a single PI controller can lead to inadequate tracking performance. Therefore, the use of additional PI controllers, in parallel with the fundamental frequency PI, tracking specific frequencies will be necessary. This issue will be further investigated in the following section.

IV. Simulation Results

This section presents simulation results using the DT-IPMSM model in Fig. 1 whose main characteristics are shown in Table I.

The proposed control strategies will be first analyzed in Simulink. An analytical model of the test machine is built to simulate its dynamic behavior. To find the most convenient combination of parallel PI controllers, different options will be compared. When Method 1 is used [see (6)-(9)], current components at $\pm 2\omega_r$ are expected in i_{dq1} and i_{dq2} (apart from the fundamental one). Therefore the use of parallel PI controllers tracking components at $\pm 2\omega_r$ as well as the fundamental one could be advantageous. Table II shows the current ripple (peak to peak) of both i_{dT} and i_{qT} when a single PI controller tracking the fundamental component of current is used and when parallel controllers tracking components at $-2\omega_r$, $+2\omega_r$ and $\pm 2\omega_r$ are added respectively. It can be observed that the addition of parallel controllers clearly improves the performance of the control strategy in terms of current ripple compared to the case in which a single PI controller tracking the fundamental component is used, the best results are obtained when additional PI controllers tracking components at $\pm 2\omega_r$ are used.

Equations (14) and (15) show that, when using Method 2, the current references in the healthy three-phase set during an open-phase fault depend on the current error in the faulty three-phase set (where no FTC is applied). Fig. 3a shows the FFT of ei_{d1} during the event of an open phase fault in phase-a. It can be observed that components at $\pm 2\omega_r$ and $\pm 4\omega_r$ have significant amplitude. Fig. 3b shows analogous results to Fig. 3a for ei_{q1} the same conclusions hold. Therefore the use of parallel PI

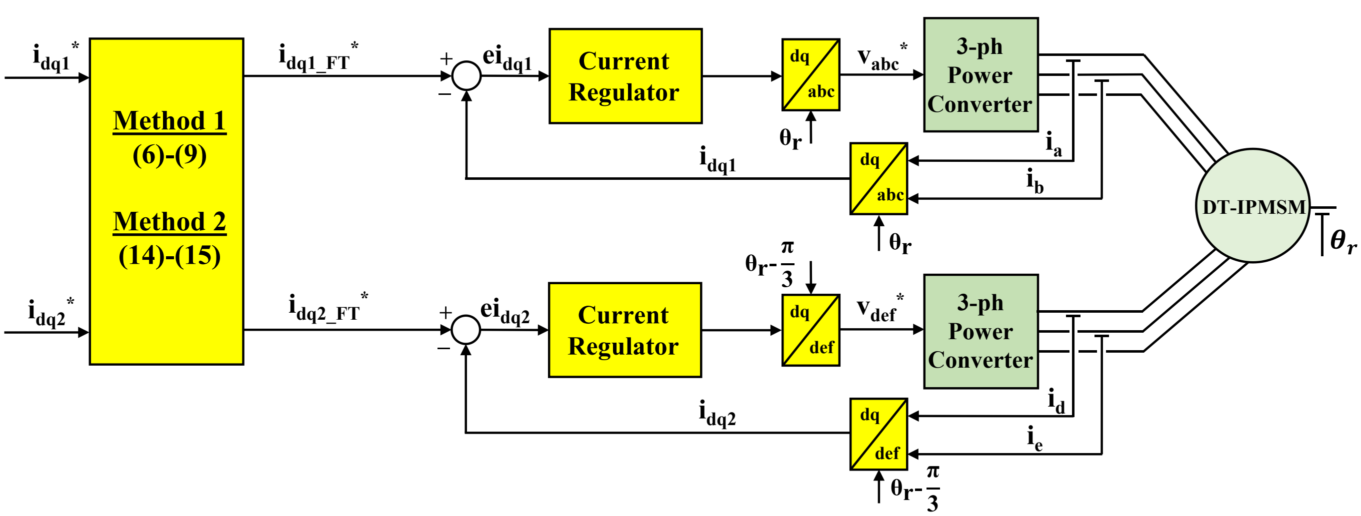

Fig. 2: Block diagram for implementation of Method 1 and Method 2.

Table II: Performance of Method 1 depending on the parallel PI controllers used			
Number of PIs	Tracked frequencies	Ripple of i_{dT}	Ripple of i_{qT}
1	Fundamental	3.6178 A	4.2375 A
2	Fundamental $-2\omega_r$	1.7828 A	1.7164 A
2	Fundamental $+2\omega_r$	3.49 A	3.5074 A
3	Fundamental $\pm 2\omega_r$	0.0228 A	0.0188 A

ω_r=1125 rpm, $i_{d1}=i_{d2}$=0A, $i_{q1}=i_{q2}$=10A

Table III: Performance of Method 2 depending on the parallel PI controllers used			
Number of PIs	Tracked frequencies	Ripple of i_{dT}	Ripple of i_{qT}
1	Fundamental	3.7727 A	4.3327 A
2	Fundamental $-2\omega_r$	1.7202 A	1.7706 A
2	Fundamental $+2\omega_r$	3.6028 A	3.8 A
3	Fundamental $\pm 2\omega_r$	1.0822 A	1.0155 A
4	Fundamental $\pm 2\omega_r$ $-4\omega_r$	0.2590 A	0.2685 A
4	Fundamental $\pm 2\omega_r$ $+4\omega_r$	0.8043 A	0.7763 A
5	Fundamental $\pm 2\omega_r$ $\pm 4\omega_r$	0.1303 A	0.1192 A

ω_r=1125 rpm, $i_{d1}=i_{d2}$=0A, $i_{q1}=i_{q2}$=10A

controllers tracking components at $\pm 2\omega_r$ and $\pm 4\omega_r$ as well as the fundamental one in the healthy three-phase set could be advantageous in this case. Table III shows the same results that Table II for Method 2, note that the use of parallel PI controllers tracking components at $\pm 4\omega_r$ has been also included in this case. It can be observed that the minimum current ripple for both i_{dT} and i_{qT} is obtained when parallel PI controllers tracking frequencies at $\pm 2\omega_r$, and $\pm 4\omega_r$ are used.

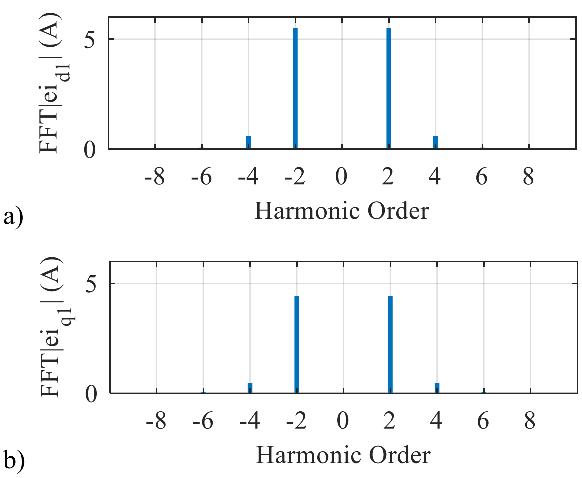

Fig. 3: FFT of a) ei_{d1} and b) ei_{q1} during an open phase fault in phase-a, **ω_r=1125 rpm, $i_{d1}=i_{d2}$=0A, $i_{q1}=i_{q2}$=10A**

From the previous discussion, it can be concluded that when Method 1 is used, the use of parallel PI controllers tracking components at $\pm 2\omega_r$ provides the best results in terms of current ripple. Otherwise, if Method 2 is applied, parallel PI controllers tracking components at $\pm 2\omega_r$, and $\pm 4\omega_r$ are required to optimize the performance of the control strategy. In addition, it can be observed that the minimum current ripple obtained with Method 2 is more than 5 times higher than that of Method 1 both for i_{dT} and i_{qT}. However, the main advantage of Method 2 is that it only requires applying the FTC strategy to the healthy three-phase set.

Once the most convenient combination of parallel PI controllers has been deduced for both Method 1 and Method 2, FEA simulations will be run to verify the validity of the proposed methods with higher accuracy. Co-simulations between Simulink and Maxwell 2D were used for this purpose. The proposed control strategy is implemented in Simulink while the electric and magnetic simulation of the test machine (see Fig. 1) under the resulting voltage commands is carried out by Ansys Maxwell 2D. Fig. 4 shows simulation results for Method 1. Initially ($t < 0.1$ s), the machine is running in healthy condition. Then, phase-a is opened at $t = 0.1$ s. It can be observed that, after the open-phase fault, current pulsations begin to appear in the *dq*-axes current of the faulty three-phase set (see Fig. 4a). However, since Method 1 is applied, current references in both three-phase sets are recalculated [see (6)-(9)] so opposite current pulsations are commanded in i_{dq2} (see Fig. 4b). Therefore, after a brief transient, i_{dqT} recovers despite the open-phase fault (see Fig. 4c). Moreover, the electromagnetic torque is seen to follow a similar tendency of that of i_{qT}, a slight increase in the amplitude of the torque ripple after the fault can be observed (see Fig. 4d). At $t = 0.3$ s, the rotating speed is increased to the machine rated value to check the performance of the method is not affected by the speed variation (see Figs. 4a-d). Finally, at $t = 0.6$ s the rotor speed is increased to 1500 rpm, which exceeds the machine rated value. Therefore, FW operation is required. In this way, negative i_{d1} and i_{d2} references (average) are commanded (see Fig. 4a-b) and i_{dT} reaches the desired value without current pulsations (see Fig. 4c). Due to this, the torque amplitude is reduced, as expected (see Fig. 4d). Moreover, Fig. 4e shows how the amplitude of the phase voltages is kept below the maximum (300V) in steady state despite the speed increase. It can be concluded that the performance of Method 1 is not affected by speed variations and allows the implementation of FW techniques. Fig. 5 shows analogous results to Fig. 4 using Method 2. It can be observed that the results obtained in Fig. 5 for Method 2 are equivalent to those obtained in Fig. 4 for Method 1, the same conclusions can be therefore reached.

V. Conclusions

Multi-phase machines provide several advantages compared to the conventional three-phase ones, especially in aspects related to the fault-tolerant capability of the machine. Among the diverse types of multi-phase machines, those with independent three-phase windings allow easier controllability since the conventional three-phase control can be applied and conventional three-phase converters can be used. Open-phase

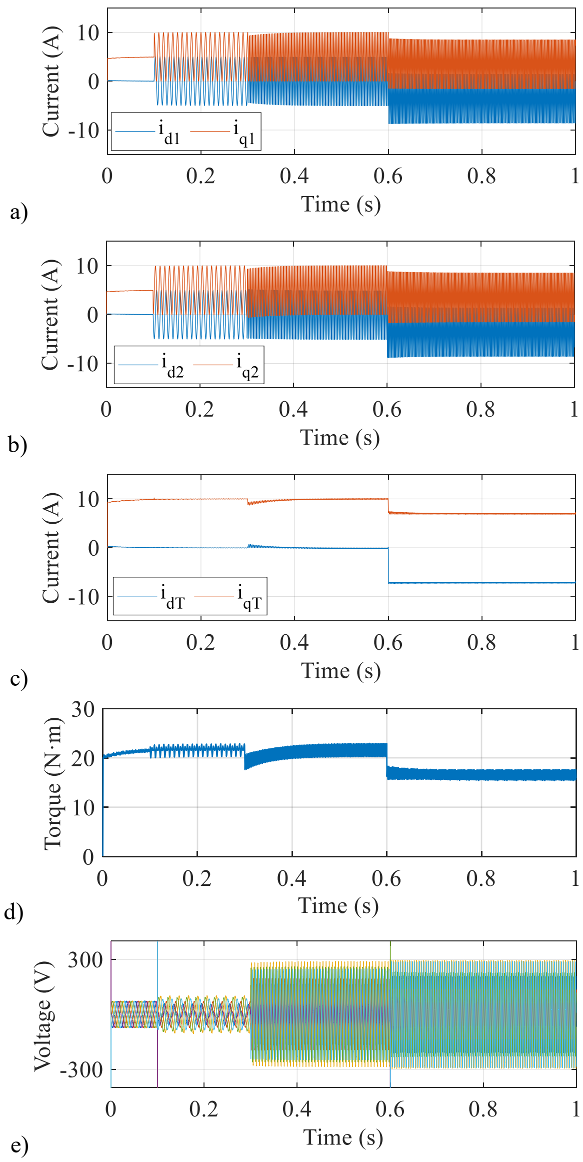

Fig. 4: a) i_{d1} and i_{q1}, b) i_{d2} and i_{q2}, c) i_{dT} and i_{qT}, d) torque and e) machine phase voltages. **$t < 0.1$s, $\omega_r = 375$ rpm, $0.1 < t < 0.6$s, $\omega_r = 1125$ rpm, $t > 0.6$s, $\omega_r = 1500$ rpm.**

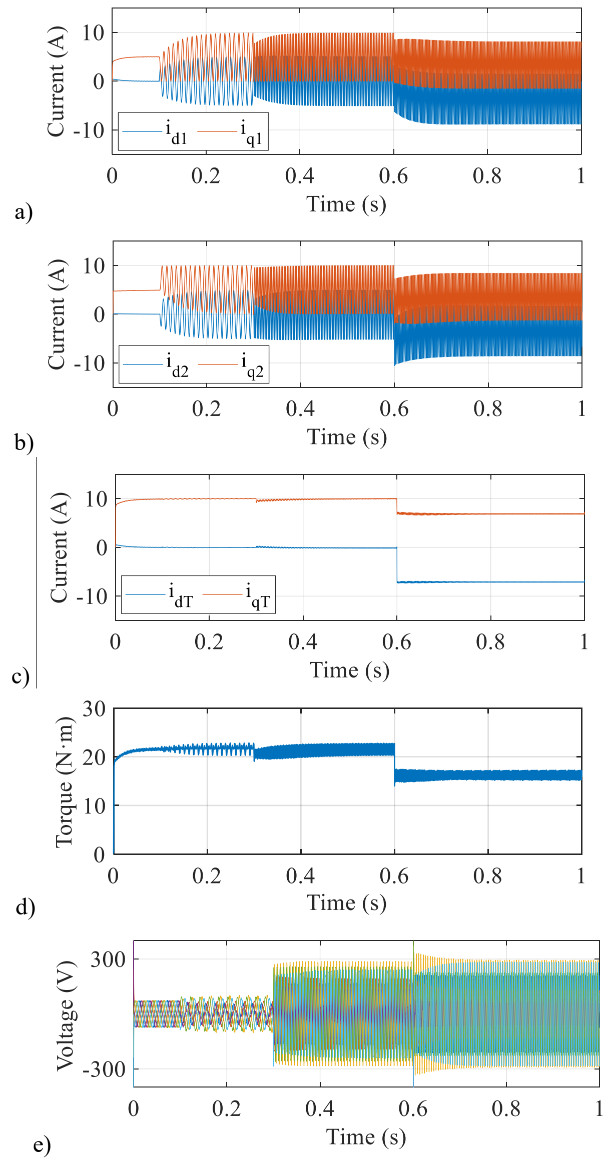

Fig. 5: Analogous results to Fig. 4 using Method 2.

faults are one of the most typical faults in electrical drives, several FT control strategies against this type of fault have been recently proposed for multi-phase machines with independent three-phase sets. This paper proposes two different FTC methods (Method 1 and Method 2) to allow continuous operation of a DT-IPMSM with isolated neutral points after an open phase fault. Both techniques are based on compensating the current pulsations that appear in the faulty three-phase set with the healthy one. Their main advantage compared with the already existing methods is the possibility of having constant and different from zero total *d*-axis currents, enabling FW and MTPA operation. Moreover, since open-phase faults lead to current pulsations in the synchronous reference frame, the use of additional parallel PI controllers tracking specific frequency components is proposed. Simulation of an analytical model of the test machine under the proposed control strategies has been performed in Simulink to find the most convenient combination of parallel PI controllers for each method. It was found that for Method 1 the use of parallel PI controllers tracking frequencies at $\pm 2\omega_r$ as well as the fundamental component was advantageous, while in Method 2, including PI controllers tracking frequencies at $\pm 2\omega_r$ and $\pm 4\omega_r$ (apart from the fundamental component) was the best option. Then, an FEA co-simulation between Simulink (control) and Ansys Maxwell 2D (machine electric/magnetic analysis) using the previously obtained combination of controllers has been used to verify the effectiveness of the proposed methods with improved accuracy. It was observed that the performance of both Method 1 and Method 2 was not affected by speed variations (below and over the machine rated value) or the implementation of FW techniques.

References

[1] X. Kestelyn and E. Semail, "A Vectorial Approach for Generation of Optimal Current References for Multiphase Permanent-Magnet Synchronous Machines in Real Time," in IEEE Transactions on Industrial Electronics, vol. 58, no. 11, pp. 5057-5065, Nov. 2011, doi: 10.1109/TIE.2011.2119454.

[2] N. Bianchi, S. Bolognani and M. Dai Pre, "Strategies for the Fault-Tolerant Current Control of a Five-Phase Permanent-Magnet Motor," in IEEE Transactions on Industry Applications, vol. 43, no. 4, pp. 960-970, July-aug. 2007, doi: 10.1109/TIA.2007.900445.

[3] H. Zhang et al., "Torque Optimization of a Seven-Phase Bi-harmonic PMSM in Healthy and Degraded Mode," 2019 22nd International Conference on Electrical Machines and Systems (ICEMS), 2019, pp. 1-6, doi: 10.1109/ICEMS.2019.8921839.

[4] A. Ashoush, S. M. Gadoue, A. S. Abdel-Khalik and A. L. Mohamadein, "Current optimization for an eleven-phase induction machine under fault conditions using Genetic Algorithm," 8th IEEE Symposium on Diagnostics for Electrical Machines, Power Electronics & Drives, 2011, pp. 529-534, doi: 10.1109/DEMPED.2011.6063674.

[5] F. Lin, Y. Hung and M. Tsai, "Fault-Tolerant Control for Six-Phase PMSM Drive System via Intelligent Complementary Sliding-Mode Control Using TSKFNN-AMF," in IEEE Transactions on Industrial Electronics, vol. 60, no. 12, pp. 5747-5762, Dec. 2013, doi: 10.1109/TIE.2013.2238877.

[6] M. Kozovsky, et al, "Verification of nine-phase PMSM model in d-q coordinates with mutual couplings," 2016 6th IEEE International Conference on Control System, Computing and Engineering (ICCSCE), 2016, pp. 73-78, doi: 10.1109/ICCSCE.2016.7893548.

[7] Fan, Linhui & Yang, Tao & Rashed, M. & Bozhko, S.. (2018). Sensorless Control Of Dual-Three Phase PMSM Based Aircraft Electric Starter/Generator System Using Model Reference Adaptive System Method. 64 (8 pp.)-64 (8 pp.). 10.1049/cp.2018.0138.

[8] S. Maekawa, et al, "Proposal of Electrolytic Capacitor-less and Reactor-less drive system using triple three phase PMSM," 2019 21st European Conference on Power Electronics and Applications (EPE '19 ECCE Europe), 2019, pp. P.1-P.6, doi: 10.23919/EPE.2019.8914922.

[9] H. S. Che et al "Postfault Operation of an Asymmetrical Six-Phase Induction Machine With Single and Two Isolated Neutral Points," in IEEE Transactions on Power Electronics, vol. 29, no. 10, pp. 5406-5416, Oct. 2014, doi: 10.1109/TPEL.2013.2293195..

[10] X. Wang, et al "Comprehensive Diagnosis and Tolerance Strategies for Electrical Faults and Sensor Faults in Dual Three-Phase PMSM Drives," in IEEE Transactions on Power Electronics, vol. 34, no. 7, pp. 6669-6684, July 2019, doi: 10.1109/TPEL.2018.2876400.

[11] Y. Hu, Y. Feng and X. Li, "Fault-tolerant Hybrid Current Control of Dual Three-phase PMSM with One Phase Open," in IEEE Journal of Emerging and Selected Topics in Power Electronics, doi: 10.1109/JESTPE.2020.3032668.

[12] X. Wang, et al, "Fault-Tolerant Control of Dual Three-Phase PMSM Drives With Minimized Copper Loss," in IEEE Transactions on Power Electronics, vol. 36, no. 11, pp. 12938-12953, Nov. 2021, doi: 10.1109/TPEL.2021.3076509.

[13] G. Feng et al, "Open-Phase Fault Modeling and Optimized Fault-Tolerant Control of Dual Three-Phase Permanent Magnet Synchronous Machines," in IEEE Transactions on Power Electronics, vol. 34, no. 11, pp. 11116-11127, Nov. 2019, doi: 10.1109/TPEL.2019.2900599.

[14] M. Shamsi-Nejad et al, "Fault Tolerant and Minimum Loss Control of Double-Star Synchronous Machines Under Open Phase Conditions," in IEEE Transactions on Industrial Electronics, vol. 55, no. 5, pp. 1956-1965, May 2008, doi: 10.1109/TIE.2008.918485.

[15] W. Wang et al, "Fault-Tolerant Control of Dual Three-Phase Permanent-Magnet Synchronous Machine Drives Under Open-Phase Faults," in IEEE Transactions on Power Electronics, vol. 32, no. 3, pp. 2052-2063, March 2017, doi: 10.1109/TPEL.2016.2559498.